

Photoluminescence modification by high-order photonic bands in $\text{TiO}_2/\text{ZnS}:\text{Mn}$ multilayer inverse opals

Jeffrey S. King, Elton Graugnard, and Christopher J. Summers^{a)}
*School of Materials Science and Engineering, Georgia Institute of Technology,
 Atlanta, Georgia 30332-0245*

(Received 10 May 2005; accepted 10 January 2006; published online 23 February 2006)

The formation of multilayered inverse opal photonic crystals by atomic layer deposition has been investigated, and shown to provide a flexible and precise technique to control the properties of photonic crystals. Inverse opals were formed by infiltration of SiO_2 opal templates with conformal layers of $\text{ZnS}:\text{Mn}$ and TiO_2 , followed by etching. The optical properties were further tuned by backfilling the structures with TiO_2 . The high-order band structure and its influence on the photoluminescent properties were studied and modification of the Cl^- and Mn^{2+} emission peaks at 460 and 585 nm were demonstrated, respectively. © 2006 American Institute of Physics.

[DOI: 10.1063/1.2177351]

For the past decade and a half, photonic crystals (PCs) have been investigated for their potential to confine and guide light. Their most defining characteristic, the photonic band gap (PBG) can be manipulated to modify many optical phenomena. For example, the radiative recombination rate, intensity, spectral emission properties, and the nanoscale routing of light can be all strongly influenced by optical confinement within these structures. The infiltration of synthetic opals and formation of inverse opals has been established as a promising method for PC fabrication.^{1–8} Several studies have demonstrated modification of spontaneous emission in opal and inverse opal structures using the pseudo-PBG (PPBG) between the second- and third-photonic bands.^{6,9–11} However, the high-order bands offer greater potential for spontaneous emission modification, from suppression due to formation of gaps, to enhancement at band edges, where the bands are flattened and exhibit low group velocity.¹²

To date, most investigations of the inverse opal structure have addressed only single infiltration material architectures. However, more complex multilayered structures can be used to increase the functionality of the structure.^{13,14} For example, for phosphor applications, there are no transparent luminescent materials with high enough refractive indices to form a full PBG. However, the combination of luminescent and high refractive index materials offers an attractive solution. High index inverse opals have been coupled with luminescent materials by nanoparticle infiltration, but it is difficult to control the precision and uniformity of the infiltration with this method.¹⁰

In contrast, atomic layer deposition (ALD) yields highly conformal growth and nanometer-scale film thickness control, and has proven to be an ideal route for opal infiltration.^{7,15} Recently, we reported successful inverse opal fabrication using ALD of $\text{ZnS}:\text{Mn}$ and TiO_2 .^{1,7,14,16} When doped, ZnS is highly luminescent with a wide range of emission wavelengths. However, its refractive index is too low for the formation of a full PBG but high enough to produce several PPBGs. TiO_2 has a higher refractive index than ZnS , but no appreciable luminescence.¹⁷ In this letter, we report the application of ALD to sequentially grow layers of lumi-

nescent ($\text{ZnS}:\text{Mn}$) and high index (TiO_2) materials to form multilayered inverse opals, and to manipulate the high-order photonic band properties to modify luminescence.

For this study, 10 μm thick opals were formed on silicon substrates by sedimentation of 466 nm silica spheres in a confinement cell, resulting in face-centered-cubic films with the (111) plane oriented parallel to the substrate.¹⁸ The structures were sintered in air at 800 °C for 2 h, and the opal void space then infiltrated using a flow-style hot-wall ALD reactor, as described elsewhere.^{1,7,14,16} The $\text{ZnS}:\text{Mn}$ infiltrations were performed at 500 °C, to thicknesses of both 10 and 20 nm, and the remaining interstitial volume in the opals was then filled with amorphous TiO_2 at 100 °C, thus creating two-layer infiltrated opals. To convert the TiO_2 to the polycrystalline anatase phase, a 400 °C, heat treatment was performed under N_2 .¹ The surface was ion milled to expose the silica template, which was removed with HF to form a stable two-layer inverse opal. The necking induced by the sintering resulted in the formation of channels between the air spheres, and ALD was used to backfill the inverse opal with up to 10 nm of amorphous TiO_2 , thus forming a three-layer luminescent inverse opal.

Figure 1(a) is a cross section of a (111) plane in a three-

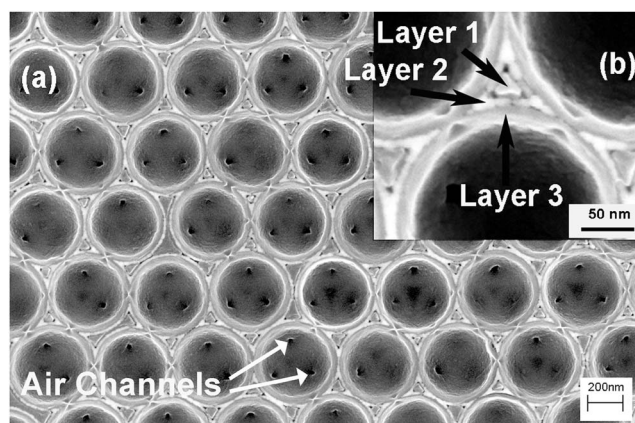


FIG. 1. (a) Ion milled cross section of the (111) plane of a 466 nm (sphere diameter) $\text{TiO}_2/\text{ZnS}:\text{Mn}/\text{TiO}_2/\text{air}$ (26/10/10 nm) layered inverse opal PC. (b) Higher magnification, Layer 1: 26 nm TiO_2 , Layer 2: 10 nm $\text{ZnS}:\text{Mn}$, Layer 3: 10 nm TiO_2 .

^{a)}Electronic mail: chris.summers@mse.gatech.edu

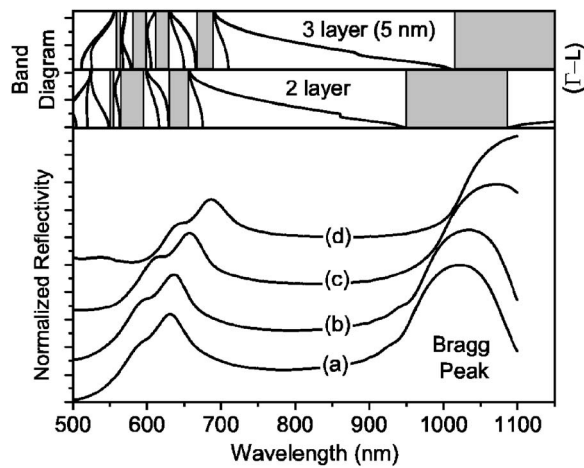


FIG. 2. Reflectivity spectra for the 466 nm (a) $\text{TiO}_2/\text{ZnS:Mn}/\text{air}$ (16/20 nm) inverse opal, and after backfilling with (b) 1, (c) 3, and (d) 5 nm. Lower and upper photonic band diagrams correspond to curves (a) and (d), respectively, with positions of the band gaps in the Γ -L direction between the second and third, as well as higher-order bands. Curves shifted vertically for clarity. 1100 nm limit due to spectrometer used (Beckman DU640). (15° from normal)

layer inverse opal. This structure had a 26 nm thick TiO_2 layer, a 10 nm thick ZnS:Mn layer, and a 10 nm thick backfilled TiO_2 layer. To highlight the multiple layers, the structure was purposely ion milled to below one-half of the opal sphere diameter, so the layers in the scanning electron microscope image do not represent the exact layer thicknesses. Figure 1(b) (inset), at higher magnification, clearly shows three distinct layers. In the images, the layers labeled “1” and “3” are TiO_2 , and “Layer 2” is ZnS:Mn . The images show that abrupt interfaces were formed, and that the layers penetrated into the sharp corners of the structure. All layers were highly conformal and spatially distinct, confirming that a multilayer inverse opal was successfully formed. X-ray data also confirmed the presence of only the ZnS and TiO_2 phases.

Figure 2 shows the specular reflectivity for a two-layer inverse opal and after each backfilling step. This structure had a 16 nm thick TiO_2 layer, a 20 nm thick ZnS:Mn layer, a 5 nm TiO_2 backfilled layer. The photonic band diagrams for the two layer and backfilled structures were calculated using the plane-wave expansion method and show the position of the PPBG between the second and third bands, as well as high-order gaps.¹⁹ The feature in the band diagram at 850 nm is due to the use of a higher dielectric constant ($\epsilon = 5.62$ and 6.08 above and below 850 nm, respectively) in the calculations for shorter wavelengths. Prior to backfilling, the (111) Bragg peak, which corresponds to the PPBG between the second- and third-photonic bands, was centered at 1022 nm, as shown in Fig. 2(a). The peak shows excellent agreement with the calculated band-gap positions. Backfilling the air voids with 1, 3, and 5 nm of TiO_2 shifted the Bragg peak to 1034, 1070, and ~ 1100 nm, respectively (Curves b–d), still showing excellent agreement with the calculated gap position.

The peak shown in Fig. 2(a), centered at ~ 600 nm, is attributed to the existence of high-order band gaps. The calculated gap positions are indicated by the shaded boxes in the figure, and the reflectivity agreed well with the calculated band structure. Curves (b–d) show the shift of the high-order band gaps with increasing backfilling. The high-order reflectivity peaks measured before TiO_2 backfilling were located at 590 nm and 630 nm, with gap edges of 550 nm to 670 nm. These peaks were found to shift with each backfilling sequence, ultimately moving to 645 and 687 nm, with gap edges of 600 and 720 nm after 5 nm of TiO_2 deposition. The peak movement observed indicates that the PPBGs between the fifth and sixth and eighth and ninth bands shifted to longer wavelengths after backfilling, agreeing with the predicted shifts.

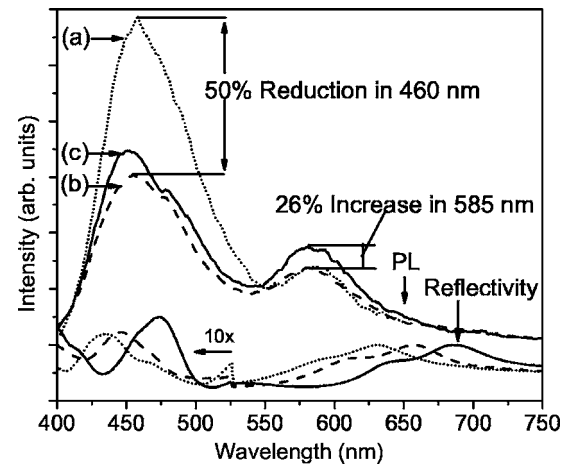


FIG. 3. PL (upper curves) compared with specular reflectivity (lower curves) as measured for (a) TiO_2 (16 nm)/ ZnS:Mn (20 nm)/air 466 nm inverse opal and after backfilling with (b) 3 and (c) 5 nm of TiO_2 .

Photoluminescence (PL) was measured on the structures described in Fig. 2 using 45° incident 337 nm pulsed ultraviolet (UV) excitation. The PL was collected normal to the (111) surface after backfilling the inverse opal as shown in Fig. 3, which shows the data from the 2 layer structure as well as the 3 nm and 5 nm backfilled structures. The corresponding reflectivity data are included for comparison, with data below 525 nm scaled 10 \times . Emission peaks were observed at both 460 nm and 585 nm, corresponding to Cl^- defect donor-acceptor and Mn^{2+} luminescent center emission, respectively. Exact comparison between the PL curves is not possible, due to variation in laser intensity between runs, and increasing TiO_2 content, which causes attenuation of the excitation photons, but is not expected to significantly affect emission. The absorption coefficient for ALD deposited amorphous TiO_2 was measured to be insignificant until below 400 nm.²⁰ In order to compare the data, the curves were normalized so that the intensities at long wavelengths (beyond 700 nm) were constant. With backfilling, significant changes were observed in both peaks, with the 460 nm peak intensity decreasing, and the 585 nm peak intensity increasing. As shown in the lower curves of the figure, high-order peaks were observed at 430 nm, as well as 625 nm. With backfilling, these peaks shifted to longer wavelengths, ultimately to 460 nm and 675 nm. The higher-energy peak shifted on top of the 460 nm peak, while the lower-energy peak shifted off of the 585 nm peak. The changes in the PL of these two peaks is thus attributed to this band gap shift.

In summary, we have reported the precise, controllable, tuning of PC optical properties using ALD of ZnS:Mn and TiO_2 . By sequentially layering these two materials, we have demonstrated an unprecedented level of independent control over the luminescence and refractive index, and thus the PBG properties of multilayer multicomponent three-

dimensional inverse opal PCs. It was shown that ALD allows formation of a composite structure through backfilling of a two-layer inverse opal with a layer of high index material, resulting in the ability to fine-tune the effective refractive index of the PC, as manifested by the shifting of the primary and high-order Γ - L band-gap peaks. In addition, higher filling fractions of high index material were possible than in the normal inverse opal configuration. Modulation of the spontaneous emission characteristics due to directional band-gap and edge effects were observed by tuning the high-order PPBG using 1–5 nm of backfilled TiO_2 , resulting in a decrease in the 460 nm peak intensity and an increase in the 585 nm peak intensity in the $\langle 111 \rangle$ direction of the PC. The data demonstrate that multilayer infiltrations using ALD uniquely enable the formation and tuning of a new class of high-quality inverse opals that independently exhibit both high index and luminescence.

This work was supported by the U.S. Army Research Office under MURI (Contract No. DAAD19-01-1-0603).

- ¹J. S. King, E. Graugnard, and C. J. Summers, *Adv. Mater. (Weinheim, Ger.)* **17**, 1010 (2005).
- ²J. E. G. J. Wijnhoven and W. L. Vos, *Science* **281**, 802 (1998).
- ³A. Blanco, E. Chomski, S. Grachtak, M. Ibisate, S. John, S. W. Leonard, C. Lopez, F. Meseguer, H. Miguez, J. P. Mondla, G. A. Ozin, O. Toader, and H. M. van Driel, *Nature (London)* **405**, 437 (2000).
- ⁴Y. A. Vlasov, X.-Z. Bo, J. C. Sturm, and D. J. Norris, *Nature (London)* **414**, 289 (2001).
- ⁵H. M. Yates, W. R. Flavell, M. E. Pemble, N. P. Johnson, S. G. Romanov, and C. M. Sotomayor-Torres, *J. Cryst. Growth* **170**, 611 (1997).
- ⁶S. G. Romanov, A. V. Fokin, and R. M. De La Rue, *Appl. Phys. Lett.* **74**, 1821 (1999).
- ⁷J. S. King, C. W. Neff, C. J. Summers, W. Park, S. Blomquist, E. Forsythe, and D. Morton, *Appl. Phys. Lett.* **83**, 2566 (2003).
- ⁸B. H. Juarez, M. Ibisate, J. M. Palacios, and C. Lopez, *Adv. Mater. (Weinheim, Ger.)* **15**, 319 (2003).
- ⁹A. Blanco, C. Lopez, R. Mayoral, H. Miguez, F. Meseguer, A. Mifsud, and J. Herrero, *Appl. Phys. Lett.* **73**, 1781.
- ¹⁰P. Lodahl, A. F. van Driel, I. S. Nikolaev, A. Irman, K. Overgaag, D. L. Vanmaekelbergh, and W. L. Vos, *Nature (London)* **430**, 654 (2004).
- ¹¹S. G. Romanov, T. Maka, C. M. S. Torres, M. Muller, and R. Zentel, *Appl. Phys. Lett.* **79**, 731 (2001).
- ¹²K. Sakoda, *Optical Properties of Photonic Crystals*, 1st ed. (Springer, New York, 2001), p. 223.
- ¹³F. Garcia-Santamaria, M. Ibisate, I. Rodriguez, F. Meseguer, and C. Lopez, *Adv. Mater. (Weinheim, Ger.)* **15**, 788 (2003).
- ¹⁴J. S. King, D. Heineman, E. Graugnard, and C. J. Summers, *Appl. Surf. Sci.* **244**, 511 (2005).
- ¹⁵A. Ruge, J. S. Becker, R. G. Gordon, and S. H. Tolbert, *Nano Lett.* **3**, 1293 (2003).
- ¹⁶J. S. King, C. W. Neff, S. Blomquist, E. Forsythe, D. Morton, and C. J. Summers, *Phys. Status Solidi B* **241**, 763 (2004).
- ¹⁷E. D. Palik, *Handbook of Optical Constants of Solids* (Academic, San Diego, 1998).
- ¹⁸S. H. Park, D. Qin, and Y. Xia, *Adv. Mater. (Weinheim, Ger.)* **10**, 1028 (1998).
- ¹⁹S. G. Johnson and J. D. Joannopoulos, *Opt. Express* **8**, 173 (2001).
- ²⁰D. Heineman, M. S. thesis, Georgia Institute of Technology, 2004.